Memorias del 2024 Congreso Nacional de Control Automático
8-11 de Octubre, 2024. Ciudad de México, México.

Dynamic Regressor Extension and Mixing Parameter Estimators—A Comparative Simulation Study of the Quadrotor System

H. Rodríguez-Cortés, R. Ortega and J. G. Romero

* *Departamento de Ingeniería Eléctrica y Electrónica*
Instituto Tecnológico Autónomo de México
Ro Hondo #1, Col. Progreso Tizapán CP. 01080. Alc. Álvaro Obregón, Ciudad de México
{hugo.rodriguez, romeo.ortega, jose.romerovelazquez}@itam.mx

Abstract: In this paper we present a comparative numerical simulation study of three dynamic regressor extension and mixing estimators applied to the quadrotor system. Our main objective is to compare the transient performance of these three parameter estimators a topic that plays a major role in parameter estimation tasks. Our study goes beyond verifying theoretically validated (asymptotic) properties. We delve into aspects not previously explored, such as sensitivity to tuning parameters, focusing specifically on a quadrotor dynamic model. The ultimate goal of this study is to provide useful design guidelines for the unmanned aerial vehicles community interested in utilizing these estimators.

Keywords: System identification, parameter estimators, quadrotor systems.

1. INTRODUCTION

Gain tuning for control and parameter adaptation algorithms is time-consuming. A classic example of this situation is the tuning of the gains of a simple PID controller. This task becomes even more involved when dealing with nonlinear algorithms for which we usually dispose only of asymptotic behavior guarantees. In this paper, we address this issue in relation to the particular problem of parameter estimators for a quadrotor aerial vehicle. We concentrate on high-performance *dynamic regressor extension and mixing* (DREM) estimators, which ensure excellent asymptotic convergence properties under extremely weak excitation conditions; see (Ortega, 2020) for a recent survey, with a focus on their practical implementations. DREM is a novel technique to design parameter estimators introduced in (Aranovskiy, 2017) that has attracted the attention of the identification and adaptive control community, reaching 424 citations in Google Scholar to date. The construction of DREM estimators involves two steps: **S1** Proceeding from the original vector linear regression equation (LRE), which is of the form $y = \psi^\top \theta$, with $y(t) \in \mathbb{R}, \psi(t) \in \mathbb{R}^q$ *measurable* signals and $\theta \in \mathbb{R}^q$ the vector of *unknown* parameters to be estimated, in the regressor extension step, we construct a *square matrix regressor* equation of the form $Y = \Psi\theta$, with $Y(t) \in \mathbb{R}^q, \Psi(t) \in \mathbb{R}^{q\times q}$ new measurable signals. **S2** The mixing step, which multiplies the matrix regression equation by the adjoint matrix of the matrix regressor, yielding a set of *scalar* regression equations of the form $\mathcal{Y}_i = \Delta\theta_i, i \in \bar{q}$ with $\mathcal{Y} := \text{adj}\{\Psi\}Y$ and $\Delta = \det\{\Psi\}$. This latter essential feature, which is unique to DREM, makes it a very powerful parameter estimation technique.

While the mixing step of DREM is always the same, the regressor extension is carried out by applying a vector-valued linear (possibly time-varying and infinite dimensional) operator to the original regression equation. Hence, the regressor extension can be achieved in many ways by selecting different linear operators—see (Ortega, 2021a) for a detailed discussion on this topic. The main feature requested for the regression extension operation is that it generates a matrix regression whose determinant, as shown in **S2** above, is the new regressor for the scalar regressor equations and satisfies suitable excitation properties. It has been shown that a determinant not being square integrable is a *necessary and suicient* condition for parameter convergence, with the convergence being *exponential* if and only if the determinant is persistently exciting (PE) (Sastry, 1989). It is clear that to ensure the required excitation of the determinant it is necessary to impose some excitation properties on the original vector regressor ψ, the weakest being interval excitation (IE) (Kreisselmeier, 1990; Tao, 2003). [2]

In the paper, we look at the following three high-performance DREM estimators, which ensure PE of the scalar regressor Δ—and, consequently, exponential convergence of the estimator—under the IE condition of the original vector regressor ψ. **E1** The GPEBO+DREM estimator reported in (Wang, 2023) generates the extended regressor applying the construction of the generalized parameter estimation-based observer (GPEBO) technique (Ortega, 2021b) to a classical gradient estimator. **E2** The LS+DREM estimator of (Ortega, 2022) replaces the gradient scheme with a least-squares one and exploits a well-known property of the covariance matrix reported in (de Larminat, 1984) to generate the extended regressor. **E3** The highly sophisticated DREM+GPEBO scheme, first

[1] H. Rodríguez-Cortés on sabbatical leave from Seccin de Mecatrnica, Depto. de Ingeniera Elctrica, Centro de Investigacin y de Estudios Avanzados del Instituto Politcnico Nacional. H. Rodrguez-Corts thanks the partial support of Mexican CONAHCYT under project Ciencia de Frontera CF-2023-I-551.

[2] It is important to note that it has been recently shown in (Wang, 2023, Proposition 2.3) that IE of the regressor ψ is *equivalent* to identifiability of the LRE $y = \psi^\top\theta$—so IE is a *necessary* condition for the solution (via on- or off-line estimators) of the parameter identification problem.

https://doi.org/10.58571/CNCA.AMCA.2024.038

reported in (Bobtsov, 2022) and later complemented in (Korotina, 2022), creates the extended regressor invoking Kreisselmeier's construction (Kreisselmeier, 1977) and then applies the mixing step to generate the scalar regression equation. GPEBO techniques are applied to the mixing step by tailoring *virtual dynamics* that generate new scalar regressors with guaranteed excitation properties, particularly that the regressor Δ is bounded away from zero in a longer time interval than the original. The study reported here aims to gain insight into their role in the transient behavior via detailed simulation studies with a quadrotor system and develop guidelines to facilitate their tuning. [3]

Quadroror parameter identification was addressed in (Dhaybi, 2020) using the recursive least squares algorithm with a covariance resetting loop to preserve the estimator alertness and increase the convergence rate and accuracy of the estimated parameters (Sastry, 1989, Theorem 2.4.4). Numerical and experimental evaluation using data from the Quanser quadrotor QBall-2 in a flight designed to ensure persistently exciting signals are provided. The aerodynamic parameters of the quadrotor rotational model are determined using the Comprehensive Identication from FrEquency Responses tool in reference (Yang, 2021). The result is validated using the Quanser 3-DOF hover quadrotor platform. A multivariable extremum-seeking algorithm solves the problem of nonlinear and closed-loop parameter identification for quadcopters (Liu, 2018). This algorithm ignores the prior knowledge of the input and output mapping to reduce sensitivity to initial values. The algorithm is tested using numerical simulations. In (Munguía, 2019), a method for estimating the model parameters of multi-rotor unmanned aerial vehicles through an extended Kalman filter is presented. The proposed approach identifies all model parameters using a single on-line estimation process that fuses measurements obtained directly from on-board sensors from actual flight log data. Kalman filtering and DREM methods are employed to estimate quadrotor parameters in (Kakanov, 2020). Numerical simulations support the theoretical developments. Experimental parameter estimation using two mixing procedures was reported in (Cortés-Benito, 2023).

The rest of the paper has the following structure. Section 2 presents the quadrotor dynamic model and in Section 3 we derive the LRE used for the estimation of the translational dynamics parameters. Section 4 presents the simulation study of the three DREM estimators described above. Finally, Section 5 presents some concluding remarks.

Notation. I_n is the $n \times n$ identity matrix, $\mathbf{e}_j \in \mathbb{R}^{n_y}$ is the j-th vector of n_y-dimensional Euclidean basis, and $\mathbb{R}_+$ denotes the positive real numbers . The action of a linear time-invariant (LTI) filter $\mathcal{F}(p) \in \mathbb{R}(p)$ on a signal $w(t)$ is denoted as $\mathcal{F}(p)[w]$, where $p^n[w] := \frac{d^n w(t)}{dt^n}$. All mappings are assumed smooth and all signals are differentiable and bounded.

2. THE QUADROTOR DYNAMIC MODEL

In this section we give the equations that describe the quadrotor dynamics and identify the parameter estimation task. Also, since the quadrotor is open-loop unstable we present a classical PD controller to stabilize it, which will be used in our simulation study.

2.1 Formulation of the estimation problem

Under standard assumptions, the quadrotor aerial vehicle can be modeled using the following equations (Leishman, 2014; Gómez-Casasola, 2022) for the translational dynamics

$$m\ddot{X} = mg\mathbf{e}_3 - T_T R\mathbf{e}_3 - \mu RHR^\top \dot{X}, \tag{1}$$

and the rotational dynamics

$$J\dot{\mathbf{\Omega}} = -\mathbf{\Omega} \times J\mathbf{\Omega} + M^b, \tag{2}$$

where $m > 0$ is the quadrotor mass, $X(t) \in \mathbb{R}^3$, with $X = \text{col}(x, y, z)$, is the inertial quadrotor position, g is the gravitational acceleration constant, $T_T(t) \in \mathbb{R}$ is the total thrust generated by the four rotors, $\mu > 0$ is the aerodynamic drag coefficient, $H = \text{diag}\{1, 1, 0\}$, and $R \in SO(3)$ with $SO(3) = \left\{R \in \mathbb{R}^{3\times 3} \mid R^\top R = I_3, \det(R) = 1\right\}$ is the rotation matrix from body to inertial axes. Moreover, $J = \text{diag}\{J_{xx}, J_{yy}, J_{zz}\} \in \mathbb{R}_+^{3\times 3}$ is the inertia matrix, $\mathbf{\Omega}(t) = \left[\begin{array}{ccc}\mathbf{p}(t) & \mathbf{q}(t) & \mathbf{r}(\mathbf{t})\end{array}\right]^\top \in \mathbb{R}^3$ is the rotational velocity and $M^b(t) \in \mathbb{R}^3$ is the vector of moments generated by modifying differentially the thrust of the four rotors.

Estimation objective. Assume that the states $\dot{X}$, R and $\mathbf{\Omega}$ and the body acceleration

$$a^b = \frac{1}{m}\left[-T_T\mathbf{e}_3 - \mu HR^\top \dot{X}\right] \tag{3}$$

are measurable. Moreover, consider that the control inputs T_T and M^b are available. Identify the constant parameters m, μ, and J.

2.2 A stabilizing control law

The quadrotor dynamic is open-loop unstable, so a stabilizing control law must be implemented. The following control law is a simplified version of (Lee, 2013) that stabilizes the quadrotor position X and the quadrotor yaw angle ψ at desired *constant* values X_d and ψ_d, respectively:

$$T_T = (R\mathbf{e}_3)^\top u,\ u = K_P(X - X_d) + K_D\dot{X} + g\mathbf{e}_3$$
$$M^b = -K_R e_R - K_O\mathbf{\Omega},\ e_R = \frac{1}{2}\left(\tilde{R} - \tilde{R}\right)^\vee,$$

where $\tilde{R} = R_d^\top R$, K_P, K_D, K_R, and K_O are positive definite matrices, and $(\cdot)^\vee$ is the map defined as $(\cdot)^\vee : \mathfrak{so}3 \to \mathbb{R}^3$ with $\mathfrak{so}(3) = \left\{\mathbf{S} \in \mathbb{R}^{3\times 3} \mid \mathbf{S} + \mathbf{S}^\top = 0\right\}$. Thus, for any $a \in \mathbb{R}^3$

$$S(a) = \begin{bmatrix} 0 & -a_3 & a_2 \\ a_3 & 0 & -a_1 \\ -a_2 & a_1 & 0 \end{bmatrix} \in \mathfrak{so}(3) \Rightarrow S(a)^\vee = \begin{bmatrix} a_1 \\ a_2 \\ a_3 \end{bmatrix}$$

and $a \times b = S(a)b, \forall\, b \in \mathbb{R}^3$. Finally, the following vectors are defined

$$r_{3d} = \frac{u}{|u|}, \quad r_{1d} = \left[\begin{array}{ccc}\sin(\psi_d) & \cos(\psi_d) & 0\end{array}\right]^\top$$

to synthesize the desired rotation matrix as follows

$$R_d = \left[\begin{array}{c|c|c} \frac{r_{3d} \times (r_{1d} \times r_{3d})}{\|r_{3d} \times (r_{1d} \times r_{3d})\|} & \frac{r_{1d} \times r_{3d}}{\|r_{1d} \times r_{3d}\|} & r_{3d}\end{array}\right]$$

3. DERIVATION OF THE LRE

In this section we derive LRE for the translational dynamics, that will be used in the sequel to implement the DREM estimators. The first LRE is obtained via simple algebraic manipulations of the dynamic equations (1).

For the translational dynamics we multiply from the left equation (1) by $\dot{X}^\top$ to get

$$\dot{X}^\top a^b = \frac{1}{m}T_T\dot{X}^\top\mathbf{e}_3 - \frac{\mu}{m}\dot{X}^\top HR^\top\dot{X}. \tag{4}$$

Grouping in a vector the unknown parameters we can rewrite (4) as a LRE for the *translational dynamics* as follows

[3] The choice of the names GPEBO+DREM versus DREM+GPEBO stems from the fact that in the former scheme the GPEBO action is carried out *before* the DREM operation, while in DREM+GPEBO this operations are inversed.

$$y_T = \psi_T^\top \theta_T \tag{5}$$

with

$$y_T = \dot{X}^\top a^b,\ \psi_T = \begin{bmatrix} -T_T \dot{X}^\top \mathbf{e}_3 \\ -\dot{X}^\top H R^\top \dot{X} \end{bmatrix},\ \theta_T = \begin{bmatrix} \frac{1}{m} & \frac{\mu}{m} \end{bmatrix}^\top \tag{6}$$

4. MAIN SIMULATION RESULTS

In this section we present the simulation of the three DREM-based estimators described in **E1**-**E3** of Section . In the interest of brevity, we present the plots of $\frac{\mu}{m}$ only—this because the behavior of the other parameter $\frac{1}{m}$ is always very similar.

4.1 Simulation scenario

The following parameters are considered in the simulations, $m = 1.4$kg, $\mu = 0.7$Ns/m. The controller gains are $K_P = \text{diag}\{5,5,5\}$, $K_D = \text{diag}\{12,12,12\}$, $K_R = \text{diag}\{4,4,0.4\}$ and $K_O = \text{diag}\{1.5,1.5,0.15\}$. The quadrotor initial position is $X(0) = \begin{bmatrix} 1.5 & 1.5 & 0 \end{bmatrix}^\top$, $R(0) = \text{diag}\{1,1,1\}$ it is commanded to move to the position $X_d = \begin{bmatrix} 0.8 & 0.8 & -1.5 \end{bmatrix}^\top$, $\psi_d = \pi/4$.

Figure 1 shows the time history of the quadrotor translational position and the trace of the rotation matrix. We see that while the behavior of the quadrotor position is monotonic, the rotation matrix has a clear overshoot. We recall that the regressor ψ_T given in (6), whose level of excitation determines the estimator performance, depends—via some complicated expressions—on the position velocity and the rotation matrix.

In all simulations below we depict the behavior of the estimated parameter $\hat{\theta}_{T2}$—that is the estimate of μ/m—and the scalar regressor Δ. We recall that the overall behavior of the estimates is determined by the latter function.

To assess the effect of *additive noise* in the performance of the DREM estimators we also present a simulation with noisy measurements. We recall that it Ortega (2022); Wang (2023) we show that the corresponding estimators are robust to additive noise, more precisely, that the defined bounded-input bounded-state operators *vis-à-vis* additive noise in the LRE.

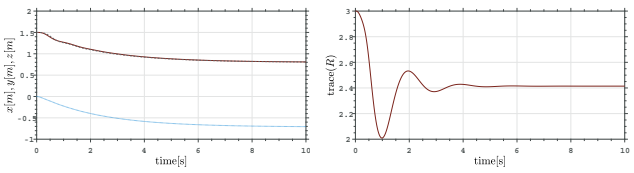

Fig. 1. Quadrotor position, (left): x (continuous line), y (dashed line), and z (dotted line). Rotation matrix trace (right).

4.2 The GPEBO+DREM estimator of **E1**

From (Wang, 2023) and the LRE (5), the GPEBO+DREM estimator for the quadrotor translational dynamic reads as

$$\begin{aligned} \dot{\hat{\theta}}_g &= -\gamma_g \psi_T (\psi_T^\top \hat{\theta}_g - y_T),\ \hat{\theta}_g(0) = \hat{\theta}_{g0} \in \mathbb{R}^2 \\ \dot{\Phi} &= -\gamma_g \psi_T \psi_T^\top \Phi,\ \Phi(0) = I_2 \\ \dot{\hat{\theta}}_T &= \gamma \Delta_{GD} \left(\mathcal{Y}_{GD} - \Delta_{GD} \hat{\theta}_T \right),\ \hat{\theta}(0) = \hat{\theta}_0 \in \mathbb{R}^2, \end{aligned} \tag{7}$$

with

$$\mathcal{Y}_{GD} = \text{adj}(I_2 - \Phi)(\hat{\theta}_g - \Phi \hat{\theta}_{g0}) \tag{8}$$

$$\Delta_{GD} = \det(I_2 - \Phi) \tag{9}$$

and γ_g, and γ the positive estimator gains.

The first simulation shown in Figure 2 considers the following gain set:

$$(\gamma_g, \gamma) \in \{(1,1), (30,1), (60,1), (100,1)\}. \tag{10}$$

The behavior for the first set of values is somehow satisfactory, with the estimate of μ/m increasing, eventually reaching the desired value (not shown in the figure.) This stems from the fact that the scalar regressor Δ_{GD} is far from zero. Interestingly, increasing γ_g (to $30, 60, 100$), drives Δ_{GD} to a small number quite close to zero, so that the estimation freezes at a value different from the correct one.

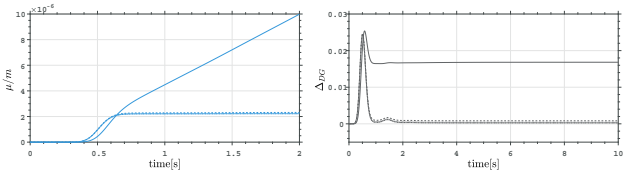

Fig. 2. Simulations for gain set (10). Estimated parameter μ/m (left). Δ_{GD} (right). $\gamma_g = 1.0$ (continuous line), $\gamma_g = 30.0$ (dashed line), $\gamma_g = 60.0$ (dotted line), and $\gamma_g = 100$ (dash-dotted line).

Motivated by the previous analysis we tried increasing γ, instead of γ_g, and simulated with the following gain set:

$$(\gamma_g, \gamma) \in \{(1,1), (1, 3\times 10^5), (1, 6\times 10^5), (1, 12\times 10^5)\}. \tag{11}$$

The results are displayed in Figure 3. We see that, starting from $\gamma = 3\times 10^5$ the estimated value reaches very fast the true one. With $(\gamma_g, \gamma) = (1,1)$ we also observed parameter convergence, but at a very slow rate—see the difference in amplitude scales between Figure 2 and Figure 3. The results depicted in Figures 2 and 3 suggest to consider the following gain set

$$(\gamma_g, \gamma) \in \{(0.5, 12\times 10^5), (1, 12\times 10^5), (1.5, 12\times 10^5), (5, 12\times 10^5)\}. \tag{12}$$

The results are presented in Figure 4, which shows that the gain γ_g modifies the convergence speed. However, by performing simulations increasing the γ_g gain, it was verified that the convergence speed settles for γ_g values larger than 10. This behavior is consistent with the Δ_{GD} values. As depicted in Figure 4, the peak in Δ_{GD} appears earlier, and the settling value is smaller when increasing the γ_g gain value.

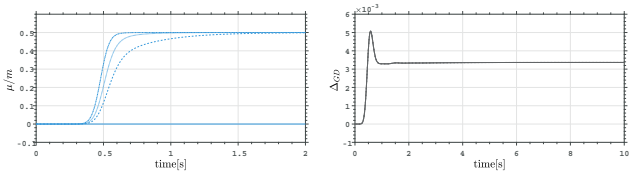

Fig. 3. Simulations for gain set (11). Estimated parameter μ/m (left), Δ_{DG} (right). $\gamma = 1.0$ (continuous line), $\gamma = 3\times 10^5$ (dashed line), $\gamma = 6\times 10^5$ (dotted line), and $\gamma = 12\times 10^5$ (dash-dotted line).

4.3 The LS+DREM estimator of **E2**

The LS+DREM of (Ortega, 2022) is described by the following equations

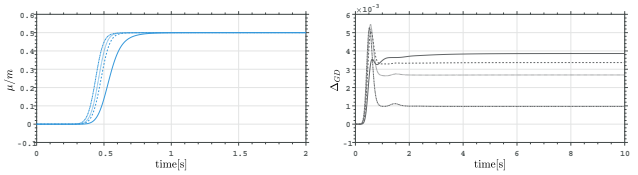

Fig. 4. Simulations for gain set (12). Estimated parameter μ/m (left), Δ_{GD}(right). $(0.5, 12 \times 10^5)$ (continuous line), $(1, 12 \times 10^5)$ (dashed line), $(1.5, 12 \times 10^5)$ (dotted line), and $(5, 12 \times 10^5)$ (dash-dotted line).

$$\begin{aligned}
\dot{\hat{\eta}} &= -\alpha F \psi_T \left(\psi_T^\top \hat{\eta} - y_T\right), \quad \hat{\eta}(0) = \eta_0 \in \mathbb{R}^2 \\
\dot{F} &= -\alpha F \psi_T \psi_T^\top F + \beta F, \quad F(0) = \frac{1}{f_0} I_2 \\
\dot{\hat{\theta}}_T &= \gamma \Delta_{LSD} \left(\mathcal{Y}_{LSD} - \Delta_{LSD} \hat{\theta}_T\right), \quad \hat{\theta}_T(0) = \theta_0 \in \mathbb{R}^2 \\
\dot{z} &= -\beta z, \quad z(0) = 1
\end{aligned} \tag{13}$$

where

$$\begin{aligned}
\Delta_{LSD} &= \det(I_2 - z f_0 F), \\
\mathcal{Y}_{LSD} &= \operatorname{adj}(I_2 - z f_0 F)(\hat{\eta} - z f_0 F \eta_0)
\end{aligned} \tag{14}$$

and we introduce a forgetting factor [4]

$$\beta = \beta_0 \left(1 - \frac{\|F\|}{M}\right). \tag{15}$$

For this estimator, the tuning gains are $\alpha > 0$, $f_0 > 0$, $\beta_0 > 0$, $M \geq \frac{1}{f_0}$ and $\gamma > 0$. As seen from the equations α plays a similar role to γ_g in the GPEBO+DREM estimator—namely, weighting the role of the first estimation stage: gradient in GPEBO+DREM and LS in LS+DREM. While γ in both estimators determines the convergence rate of the second scalar estimator.

The first simulation is performed to evaluate the role of α. Towards this end, we fix $\beta = 1.0$, $M = 1.0$, $f_0 = 2$, $\gamma = 1$ and change α to the following values $\{1, 30, 60, 120\}$. Figure 5 shows the estimator behavior for these choices. Note that the gain α amplifies the value of the signal Δ_{LSD}; thus, the parameter convergence speed increases, as illustrated in Figure 5. Although not shown in the figure in all cases parameter convergence is achieved because Δ_{LSD} converges to a non-zero value.

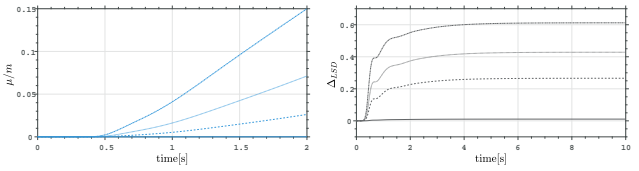

Fig. 5. Role of α with $\gamma = 1$. Estimated parameter μ/m (left), Δ_{LSD} (right). $\alpha = 1$ (continuous line), $\alpha = 30$ (dashed line), $\alpha = 60$ (dotted line), and $\alpha = 120$ (dash-dotted line).

The second simulation evaluates the effect of γ and considers the following values $\gamma = \{1, 30, 60, 120\}$. The results of this simulation are reported in Figure 6. Interestingly, the gain γ has a similar effect on the estimated parameters convergence speed as the gain α. However, the convergence speed increases much less than the speed increased by varying the gain α—notice the difference in amplitude scales. Note in Figure 6 that the gain γ does not affect the signal Δ_{LSD}. Thus, the gain γ speeds up parameter convergence differently than the gain α.

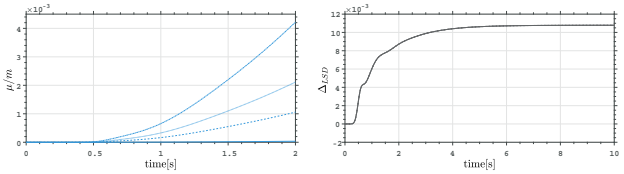

Fig. 6. Role of γ.Estimated parameter μ/m (left), Δ_{LSD} (right). $\gamma = \text{diag}\{1, 1\}$ (continuous line), $\gamma = \text{diag}\{30, 30\}$ (dashed line), $\gamma = \text{diag}\{60, 60\}$ (dotted line), and $\gamma = \text{diag}\{120, 120\}$ (dash-dotted line).

The third simulation considers the variation of the gain f_0. As seen in the definition of $F(0)$ this constant determines the initial value of the covariance matrix. A key property of the LS algorithm, that was first reported in (de Larminat, 1984), is that [5]

$$\frac{d}{dt}(F^{-1}\tilde{\eta}) = -\beta F^{-1}\tilde{\eta}. \tag{16}$$

Solving this equation we get

$$\tilde{\eta} = z f_0 F \tilde{\eta}(0). \tag{17}$$

From which it is clear that reducing f_0 reduces the estimation error. In Figure 7 we present the results for $f_0 = \{2, 5, 15, 30\}$. From the figure it is seen that increasing f_0 slows down the parameter convergence speed; this is a consequence of the decrease in scalar regressor Δ_{LSD}.

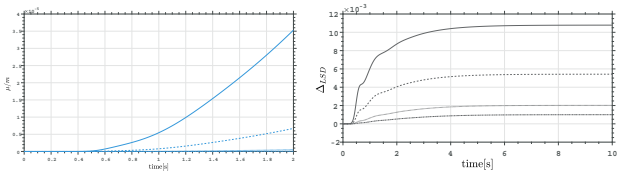

Fig. 7. Estimated parameter μ/m (left), Δ_{LSD} (right). $f_0 = 2$ (continuous line), $f_0 = 5$ (dashed line), $f_0 = 15$ (dotted line), and $f_0 = 30$ (dash-dotted line).

The fourth and fifth simulation pertain to the gains M and β_0 which are related with the forgetting mechanism that was introduced via (15). As thoroughly discussed in (Slotine, 1991, Section 8.7.6) this implements a *bounded gain* forgetting. Indeed, a zero forgetting factor leads to vanishing gain (in the face of PE) while a constant positive factor leads to exploding gain (in the absence of PE). To keep the benefits of data forgetting (parameter tracking ability) while avoiding the possibility of gain unboundedness, it is desirable to tune the forgetting factor variation so that data forgetting is activated when the regressor is PE and suspended when it is not. Since the magnitude of the covariance matrix F is an indicator of the excitation level, it is reasonable to correlate the forgetting factor variation with $\|F\|$. A specific technique for achieving this purpose is to choose the forgetting factor as (15) with β_0 and M being positive constants representing the maximum forgetting rate and prespecified bound for gain matrix magnitude, respectively. The forgetting factor β implies forgetting the data with a factor β_0 if the norm of F is small (indicating strong PE), reducing the forgetting

[4] This factor is introduced to compensate the well-known drawback of LS algorithms that, due to the covariance wind-up problem, they loose their alertness to track parameter variations (Sastry, 1989, Section 2.3.2). If this feature is removed we set $\beta = 0$.

[5] The result reported in (de Larminat, 1984) pertains to the case of LS *without* forgetting factor, that is with $\beta(t) = 0$. The equation above is then a generalization of this result.

https://doi.org/10.58571/CNCA.AMCA.2024.038

speed if $\|F\|$ becomes larger and suspends forgetting if the norm reaches the specified upper bound M.

In Figure 8 we consider the variation of the gain M within the set $\{1, 5, 15, 30\}$. As can be observed, the gain slightly increases the value of the signal Δ_{LSD}, and this effect is reflected in a slight parameter convergence speed-up. In Figure 9 we consider variations of β in the set $\{1, 10, 50, 100\}$. Note that increasing β also increases the value of Δ_{LSD} to a certain level. After this level, increasing β has a negligible effect on the Δ_{LSD} value. As expected, growing Δ_{LSD} increases the estimated parameters convergence, as illustrated in Figure 9.

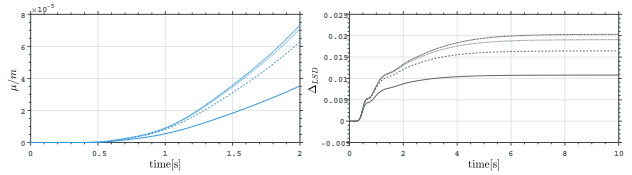

Fig. 8. Role of M. Estimated parameter μ/m (left), Δ_{LSD} (right). $M = 1$ (continuous line), $M = 5$ (dashed line), $M = 15$ (dotted line), and $M = 30$ (dash-dotted line).

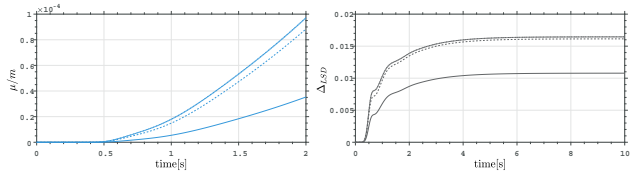

Fig. 9. Role of β. Estimated parameter μ/m (left), Δ_{LSD} (right). $\beta = 1$ (continuous line), $\beta = 10$ (dashed line), $\beta = 50$ (dotted line), and $\beta = 100$ (dash-dotted line).

Finally, the following gains are selected $\beta = 50$, $M = 1$, $f_0 = 5$, $\gamma = 60$ and $\alpha = 60$. Figure 10 shows the results together with the following gain combinations

$$(\beta, M, f_0, \gamma, \alpha) \in \{(50, 1, 5, 60, 60)_1, (50, 1, 5, 60, 120)_2, (50, 1, 5, 120, 60)_3, (50, 1, 5, 120, 120)_4\}. \quad (18)$$

Note that increasing only α positively affects the convergence speed without affecting the value of Δ_{LSD}. On the other hand, raising only γ does not change the value of Δ_{LSD}, and the convergence speed slows down. Finally, increasing both gains α and γ speeds up the convergence rate and the value of Δ_{LSD}.

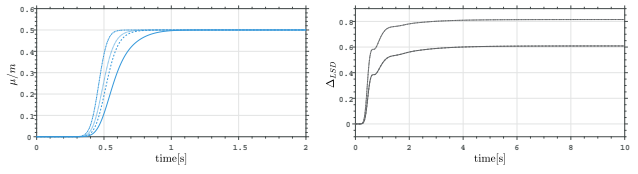

Fig. 10. Gain set (18). Estimated parameter μ/m (left), Δ_{LSD} (right). $(\cdot)_1$ (continuous line), $(\cdot)_2$ (dashed line), $(\cdot)_3$ (dotted line), and $(\cdot)_4$ (dash-dotted line)

Remark 1. As explained in (Ortega, 2022) the extended regressor in the LS+DREM estimator is created replacing the gradient estimator of (Wang, 2023) by a LS scheme and exploiting the key property of the covariance matrix F identified in (16). This allows us to derive (17) from which we can define the extended LRE

$$(\hat{\eta} - z f_0 F \eta_0) = (I_2 - z f_0 F)\theta_T,$$

to which we apply the standard mixing procedure to get the scalar LREs $\{\mathcal{Y}_{LSD}\}_i = \Delta_{LSD}\theta_{Ti}, i = 1, 2$.

4.4 The DREM+GPEBO estimator of **E3**

Following the developments reported in (Korotina, 2022), the construction of the DREM+GPEBO estimator proceeds from the translational LRE (5) and starts by constructing the Kreisselmeier regressor extension (Korotina, 2022, Proposition 1) and applying the DREM procedure to get the following scalar LREs.

$$\mathcal{Y}^1_{DG} = \Delta_{DG}\theta_{T1},\ \mathcal{Y}^2_{DG} = \Delta_{DG}\theta_{T2} \quad (19)$$

where we defined

$$\begin{aligned} Z = \mathcal{F}_1(p)\left[\psi_T y_T\right],\ \Psi = \mathcal{F}_1(p)\left[\psi_T \psi_T^\top\right] \\ \mathcal{Y}_{DG} = \text{adj}(\Psi)Z,\ \Delta_{DG} = \det(\Psi) \end{aligned} \quad (20)$$

with the filter $\mathcal{F}_1(p) = \frac{g}{p+\lambda}$, $g > 0$ and $\lambda > 0$.

We consider the scenario where Δ_{DG} does not have the required excitation properties and proceed to construct *new scalar* LRE with guaranteed PE of the new scalar regressor. Towards this end, the following dynamic systems are constructed. For θ_{T2}

$$\dot{z}_2 = \rho(\phi_{21}\mathcal{Y}^2_{DG} - z_2), \quad z_2(0) = 0 \quad (21)$$

with $\rho > 0$, and ϕ_{21}, ϕ_{22} defined as

$$\begin{aligned} \begin{bmatrix} \dot{\phi}_{21} \\ \dot{\phi}_{22} \end{bmatrix} &= \begin{bmatrix} 0 & -\rho\Delta_{DG}\phi_{21} \\ \rho\Delta_{DG}\phi_{21} & -(\frac{1}{2}(\phi^2_{21} + \phi^2_{22}) + \beta) \end{bmatrix} \begin{bmatrix} \phi_{21} \\ \phi_{22} \end{bmatrix}, \\ &\begin{bmatrix} \phi_{21}(0) & \phi_{22}(0) \end{bmatrix}^\top = \begin{bmatrix} 1 & 0 \end{bmatrix}^\top \\ \begin{bmatrix} \dot{\zeta}_{21} \\ \dot{\zeta}_{22} \end{bmatrix} &= \begin{bmatrix} 0 & -\rho\Delta_{DG}\phi_{21} \\ \rho\Delta_{DG}\phi_{21} & -(\frac{1}{2}(\phi^2_{21} + \phi^2_{22}) + \beta_2) \end{bmatrix} \begin{bmatrix} \zeta_{21} \\ \zeta_{22} \end{bmatrix} \\ &+ \begin{bmatrix} \rho_2\Delta_{DG}\phi_{21}z_2 \\ (\frac{1}{2}(\phi^2_{21} + \phi^2_{22}) + \beta_2 - \rho_2)z_2 \end{bmatrix}, \\ &\begin{bmatrix} \zeta_{21}(0) & \zeta_{22}(0) \end{bmatrix}^\top = \begin{bmatrix} 0 & 0 \end{bmatrix}^\top \end{aligned} \quad (22)$$

with $\beta > 0.5$. Invoking GPEBO, the following new LRE is synthesized based on the dynamic systems (21), and (22).

$$\bar{\mathcal{Y}}_{DG} = \bar{\Phi}\theta_T \quad (23)$$

with $\bar{\mathcal{Y}}_{DG} = z_2 - \zeta_{22}$ and $\bar{\Phi} = \psi_{22}$, and it is proven that if the original regressor ψ_T is IE we have that $\bar{\Phi}$ is PE. Thus, the classical gradient estimator

$$\dot{\hat{\theta}}_{T2} = \gamma\phi_{22}(z_2 - \zeta_{22} - \phi_{22}\hat{\theta}_{T2}) \quad (24)$$

ensures *exponential* convergence.

As seen from the derivations above, this is a highly complicated construction that involves many tuning gains, whose interpretation is far from clear. Figure 11 presents the estimator response with $\gamma = 1$, $\beta = 0.75$, and $\rho \in \{1, 30, 60, 90\}$. As seen in the figure, in all cases Δ_{DG} and ϕ_{22} converge to zero. However, ϕ_{22} is different from zero more time than Δ_{DG}, hence, ϕ_{22} has a larger exciting interval than Δ_{DG}. We recall that it is this signal that acts as regressor in the final gradient estimator (24). Also, it is clear from the figure that increasing ρ speeds-up the transient. This behavior may be explained as follows. From (21) we see that ρ_2 is the inverse of the time constant of the filter. Hence, increasing ρ_2 makes z_2 to converge faster to $\phi_{21}\mathcal{Y}^2_{DG}$. This, in its turn "speeds-up" the GPEBO stage of the algorithm.

Figure 12 depicts the estimator response with $\mu = 1$ and $\gamma \in \{1, 30, 60, 90\}$. It is again seen that Δ_{DG} converges to zero in all cases, and γ does not modify the behavior of ϕ_{22}. Also, it is

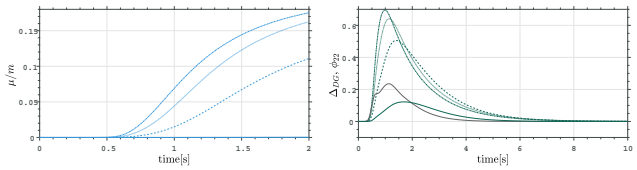

Fig. 11. Efect of ρ. Estimated parameter μ/m (top), (Δ_{DG}, ϕ_{22}-green line-) (right). $\rho = 1$ ($5 \times \Delta_{DG}, 5 \times \phi_{22}$) (continuous line), $\rho = 30$ (dashed line), $\rho = 60$ (dotted line), and $\rho = 90$ (dash-dotted line).

clear from the figure that—as expected from the equations of the gradient estimator (24)—increasing γ fastens the transient behavior. Furthermore, this transient improvement is more pronounced than the one achieved increasing ρ, which is somehow indirect.

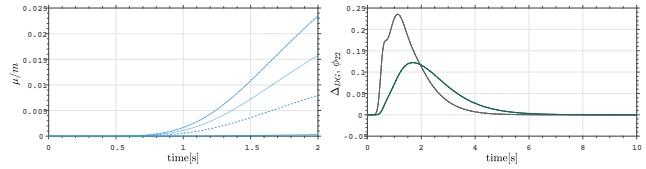

Fig. 12. Effect of γ. Estimated parameter μ/m (left), $5 \times \Delta_{DG}$, $5 \times \phi_{22}$ -green line- (right). $\gamma = 1.0$ (continuous line), $\gamma = 30.0$ (dashed line), $\gamma = 60.0$ (dotted line), and $\gamma = 90$ (dash-dotted line).

From the results in the previous simulations, the following gain combinations are tested.

$$(\gamma, \mu) \in \{(90, 30), (30, 90), (30, 120), (30, 150)\}.$$

The results are depicted in Figure 13, which shows that the best response is obtained by increasing ρ with respect to γ. Finally, it was verified that with the gain combination $(30, 150)$ there is no noticeable effect when the gain β varies.

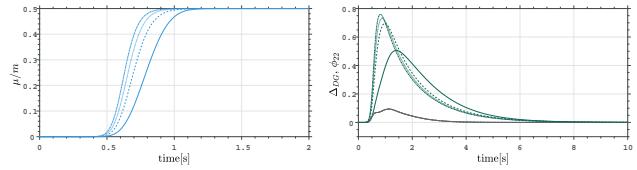

Fig. 13. Estimated parameter $1/m$ (left), Δ_{DG}, ϕ_{22} -green line-(right). $(90, 30)$ (continuous line), $(30, 90)$ (dashed line), $(30, 120)$ (dotted line), and $(30, 150)$ (dash-dotted line).

5. CONCLUDING REMARKS

With the purpose of revealing the role of the various tuning gains in three DREM estimators, we have carried out a detailed simulation study of their effect when applied for the estimation of the parameters of a quadrotor. It has been observed that the estimators response is monotonic with respect all gains changes, which significantly simplifies the tuning task . As expected, the behavior of the scalar regressors Δ_{GD}, Δ_{LSD}, and Δ_{DG} are the best indicators to monitor the effect of the gains on the estimated values.

REFERENCES

S. Aranovskiy, A. Bobtsov, R. Ortega and A. Pyrkin, Performance enhancement of parameter estimators via dynamic regressor extension and mixing, *IEEE Trans. Automatic Control*, vol. 62, pp. 3546-3550, 2017.

S. Aranovskiy, A. Belov, R. Ortega, N. Barabanov and A, Bobtsov, Parameter identification of linear time-invariant systems using dynamic regressor extension and mixing. *International Journal of Adaptive Control and Signal Processing*, vol. 33, no. 6, pp. 1016-1030, 2019.

A. Bobtsov, B. Yi, R. Ortega and A. Astolfi, Generation of new exciting regressors for consistent on-line estimation of unknown constant parameters, *IEEE Trans. Automatic Control*, vol. 67, no. 9, pp.4746-4753, 2022.

I. Cortés-Benito, Y. E. Tlatelpa-Osorio, M. Martínez-Ramrez, J. G. Romero and H. Rodríguez-Cortés, Experimental Quadrotor Physical Parameters Estimation, *2023 International Conference on Unmanned Aircraft Systems (ICUAS)*, Warsaw, Poland, pp. 1356-1362, doi: 10.1109/ICUAS57906.2023.10156332, 2023.

Ph. de Larminat, On the stabilizability condition in indirect adaptive control, *Automatica*, vol. 20, no, 6, pp. 793-795, 1984.

M. Dhaybi and N. Daher, Accurate real-time estimation of the inertia tensor of package delivery quadrotors, in *2020 American Control Conference (ACC)*, pp. 15201525, 2020

A. Gómez-Casasola and H. Rodríguez-Cortés, Scale Factor Estimation for Quadrotor Monocular-Vision Positioning Algorithms. *Sensors*, 22, 8048. https://doi.org/10.3390/s22208048, 2022.

K. Guo and Y. Pan, Composite adaptation and learning for robot control: A survey, *IFAC Annual Reviews in Control*, Vol. 55, pp. 279-290, 2023.

M. A. Kakanov, S. I. Tomashevich, V. S. Gromov, O. I. Borisov, F. B. Gromova, and A. A. Pyrkin, Parameter estimation of quadrotor model, in *2020 International Conference Nonlinearity, Information and Robotics (NIR)*, pp. 15, 2020.

M. Korotina, J. G. Romero, S. Aranovskiy, A. Bobtsov and R. Ortega, A new on-line exponential parameter estimator without persistent excitation, *Systems and Control Letters*, vol. 159, 105079, 2022.

G. Kreisselmeier, Adaptive observers with exponential rate of convergence, *IEEE Trans. Automatic Control*, vol. 22, no. 1, pp. 2-8, 1977.

G. Kreisselmeier and G. Rietze-Augst, Richness and excitation on an interval- with application to continuous-time adaptive control, *IEEE Trans. Automatic Control*, vol. 35, no. 2, pp. 165-171, 1990.

T. Lee, Robust adaptive attitude tracking on SO(3) with an application to a quadrotor UAV, *IEEE Transactions on Control Systems Technology*, vol. 21, no. 5, pp. 19241930, September 2013.

R.C. Leishman, J.C Macdonald, R.W; Beard and T.W. McLain, Quadrotors and Accelerometers: State Estimation with an Improved 392 Dynamic Model. *IEEE Control Systems Magazine*, 34, 2841. doi:10.1109/MCS.2013.2287362, 2014.

W. Liu, X. Huo, J. Liu, and L. Wang, Parameter identification for a quadrotor helicopter using multivariable extremum seeking algorithm, *International Journal of Control, Automation and Systems*, vol. 16, no. 4, pp. 195119611, 2018.

R. Munguía, S. Urzua, and A. Grau, EKF-based parameter identification of multi-rotor unmanned aerial vehiclesmodels, *Sensors*, vol. 19, no. 19, 2019.

R. Ortega, V. Nikiforov and D. Gerasimov, On modified parameter estimators for identification and adaptive control: a unified framework and some new schemes, *IFAC Annual Reviews in Control*, vol. 50, pp. 278-293, 2020.

R. Ortega, S. Aranovskiy, A. Pyrkin, A Astolfi and A. Bobtsov, New results on parameter estimation via dynamic regressor extension and mixing: Continuous and discrete-time cases, *IEEE Trans. Automatic Control*, vol. 66, no. 5, pp. 2265-2272, 2021.

R. Ortega, A. Bobtsov, N. Nikolayev, J. Schiffer and D. Dochain, Generalized parameter estimation-based observers: application to power systems and chemical-biological reactors, *Automatica*, vol. 129, 109635, 2021.

R. Ortega, J. G. Romero and S. Aranovskiy, A new least squares parameter estimator for nonlinear regression equations with relaxed excitation conditions and forgetting factor, *Systems and Control Letters*, vol. 169, no. 105377, 2022.

Y. Pan, T. Shi and R. Ortega, Comparative analysis of parameter convergence for several least-squares estimation schemes, *IEEE Trans. Automatic Control*, (DOI:10.1109/TAC.2023.3326054), 2023.

J. Romero, R Ortega and A. Bobtsov, Parameter estimation and adaptive control of EulerLagrange systems using the power balance equation parameterisation. *International Journal of Control*, 96(2), pp. 475-487, doi.org/10.1080/00207179.2021.2002935, 2021.

S. Sastry and M. Bodson, *Adaptive Control: Stability, Convergence and Robustness*, Prentice-Hall, New Jersey, 1989.

J.-J.E. Slotine and W. Li, *Applied Nonlinear Control*, Prentice-Hall, New Jersey, USA, 1991.

G. Tao, *Adaptive Control Design and Analysis*, vol. 37, John Wiley & Sons, New Jersey, 2003.

L. Wang, R. Ortega, A. Bobtsov, J. G. Romero and B. Yi, Identifiability implies robust, globally exponentially convergent on-line parameter estimation: Application to model reference adaptive control, *Int. J. of Control*, (DOI:10.1080/00207179.2023.2246595), 2023.

S. Yang, L. Xi, J. Hao, and W. Wang, Aerodynamic-parameter identification and attitude control of quad-rotor model with cifer and adaptive ladrc, *Chinese Journal of Mechanical Engineering*, vol. 34, no. 1, pp. 110, 2021.

